

Preparation, Crystal Structures, and Magnetic Features for a Series of Dinuclear $[\text{Ni}^{\text{II}}\text{Ln}^{\text{III}}]$ Schiff-Base Complexes: Evidence for Slow Relaxation of the Magnetization for the Dy^{III} Derivative

Traian D. Pasatoiu,[†] Jean-Pascal Sutter,^{*,‡,§} Augustin M. Madalan,[†] Fatima Zohra Chiboub Fellah,^{‡,§,||} Carine Duhayon,^{‡,§} and Marius Andruh^{*,†}

[†]University of Bucharest, Faculty of Chemistry, Inorganic Chemistry Laboratory, Str. Dumbrova Rosie nr. 23, 020464-Bucharest, Romania

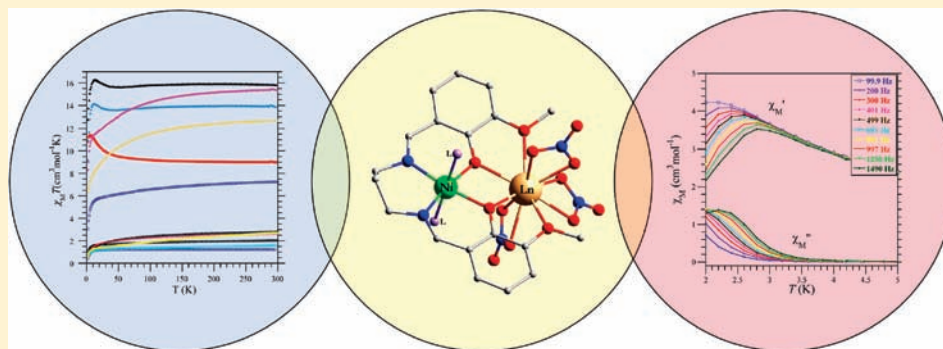
[‡]CNRS, LCC (Laboratoire de Chimie de Coordination), 205, route de Narbonne, F-31077 Toulouse, France

[§]Université de Toulouse, UPS, INPT, LCC, F-31077 Toulouse, France

^{||}Department of Chemistry, Faculty of Science, University Aboubaker Belkaid, BP 119, 13000 Tlemcen, Algeria

S Supporting Information

ABSTRACT:



A series of dinuclear $[\text{Ni}^{\text{II}}\text{Ln}^{\text{III}}]$ Schiff-base complexes (using a Schiff-base dicompartmental ligand derived from *o*-vanillin [$\text{H}_2\text{valpn} = 1,3\text{-propanediylbis}(2\text{-iminomethylene-6-methoxy-phenol})$]) with $\text{Ln} = \text{La}, \text{Ce}, \text{Pr}, \text{Nd}, \text{Sm}, \text{Eu}, \text{Gd}, \text{Tb}, \text{Dy}, \text{Ho}, \text{Er}$, and a hydroxo-bridged tetranuclear $[\text{Ni}^{\text{II}}\text{Yb}^{\text{III}}]$ are reported. The crystal structures have been solved for 10 dinuclear complexes revealing four arrangements for the dinuclear units, which are modulated by the coordinated solvent molecules and the nitrate-anion interactions. The magnetic behaviors have been investigated, and the nature of the $\text{Ni}^{\text{II}}\text{-Ln}^{\text{III}}$ exchange interaction has been emphasized by comparison with the behavior of the related $[\text{Zn}^{\text{II}}\text{Ln}^{\text{III}}]$ derivatives. This allowed for establishing that the interaction within these compounds is antiferromagnetic with the 4f ions of the beginning of the Ln series and turns ferromagnetic from Gd^{III} toward the end of the series. AC susceptibility investigations clearly show the occurrence of slow relaxation processes of the magnetization close to 2 K for the dinuclear $[\text{Ni}^{\text{II}}\text{Dy}^{\text{III}}]$ complex.

INTRODUCTION

The combination of different paramagnetic metal ions within the same molecular entity leads to a wide variety of magnetic properties of the polynuclear complexes.¹ Among these, 3d–4f complexes are a special case and have been intensively studied in order to reveal the factors governing the nature and magnitude of the exchange interaction between a 3d metal ion and various 4f metal ions.² Lanthanide ions bring large and, in some cases, highly anisotropic magnetic moments. The interest for 3d–4f heteronuclear complexes grew rapidly after Gatteschi et al.'s report on the ferromagnetic interaction between the adjacent Cu^{II} and Gd^{III} ions within trinuclear $\text{Cu}^{\text{II}}\text{Gd}^{\text{III}}\text{Cu}^{\text{II}}$ complexes.³ Nowadays, we are facing a revival of the 3d–4f combined chemistry that is due to the discovery of molecular nanomagnets,

which exhibit hysteresis in the absence of long-range magnetic order.⁴ These are the so-called single-molecule magnets (SMMs) and single-chain magnets (SCMs). Their design requires the use of lanthanides exhibiting a high anisotropy, of which the best candidates are Tb^{III} (${}^7\text{F}_6$), Dy^{III} (${}^6\text{H}_{15/2}$), and Ho^{III} (${}^5\text{H}_8$). Interestingly, a compound as simple as a dinuclear $[\text{Cu}\text{-Tb}]$ complex was found to exhibit SMM behavior, yet at very low temperature.⁵

An important breakthrough in the study of 3d–4f complexes was realized by Costes et al., who developed a general synthetic route leading to strictly dinuclear complexes.⁶ This strategy is

Received: March 2, 2011

Published: June 02, 2011

based upon the use of bicompartamental Schiff base ligands with a N_2O_2 coordination site, hosting the 3d ion, and an open O_2O_2 coordination site, able to accommodate the large 4f metal ions. The synthesis of such complexes is a stepwise process, in which the 3d ion is first introduced before the resulting complex is used as a ligand to coordinate the 4f ion.

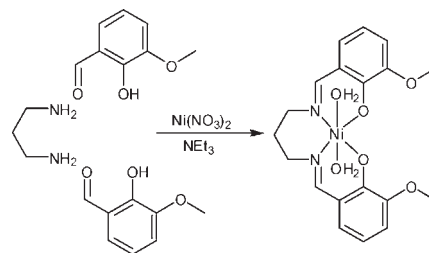
The magnetic studies of polynuclear $Cu^{II}Gd^{III}$ complexes proved that the exchange interaction within the $Cu^{II}-Gd^{III}$ pair is, in most cases, ferromagnetic.⁷ The peculiarity of the $Cu^{II}-Gd^{III}$ coupling raised further questions concerning the nature of the magnetic exchange interactions between (i) Gd^{III} and other paramagnetic 3d metal ions, (ii) Cu^{II} and the other Ln^{III} cations, and (iii) more generally $Ln(III)$ ions with other spin carriers. To address these questions, numerous 3d–4f complexes, mainly dinuclear, have been synthesized and investigated.⁷ Several bimetallic complexes containing $M^{n+}-Gd^{3+}$ pairs,⁸ such as $VO^{2+}-Gd^{3+}$,⁹ $Ni^{2+}-Gd^{3+}$,¹⁰ $Co^{2+}-Gd^{3+}$,¹¹ $Cr^{3+}-Gd^{3+}$,¹² $Fe^{2+/3+}-Gd^{3+}$,¹³ were studied. Both ferro- and antiferromagnetic interactions have been observed; moreover, geometrical factors have been found to influence the nature of the exchange coupling. Although the $M^{n+}-Gd^{3+}$ magnetic interaction was found to be ferromagnetic in many cases, examples in which this interaction is antiferromagnetic are known as well.^{8,14}

Kahn investigated the magnetic interaction in oxamato-bridged $Cu^{II}Ln^{III}$ complexes by comparison with their analogues containing a diamagnetic 3d metal ion. This led to the conclusion that $M^{II}-Gd^{III}$, $M^{II}-Tb^{III}$, and $M^{II}-Dy^{III}$ ($M^{II} = Ni^{II}, Cu^{II}$) interactions are ferromagnetic.^{15,16} Costes et al. observed with Schiff-base complexes that the $Cu^{II}-Ln^{III}$ interaction is antiferromagnetic for $Ln^{III} = Ce^{III}, Nd^{III}, Sm^{III}, Tm^{III}$, and Yb^{III} and ferromagnetic for $Ln^{III} = Gd^{III}, Tb^{III}, Dy^{III}, Ho^{III}$, and Er^{III} ,¹⁷ while Okawa et al. came to the conclusion that the interaction is antiferromagnetic for $Ln^{III} = Ce^{III}, Pr^{III}$, and Sm^{III} and ferromagnetic for $Ln^{III} = Gd^{III}, Tb^{III}, Dy^{III}, Ho^{III}$, and Er^{III} .¹⁸ Mohanta et al. studied a series of heterodinuclear $Cu^{II}-Ln^{II}$ complexes and stated that there is a ferromagnetic interaction for $Ln^{III} = Gd^{III}, Tb^{III}, Dy^{III}, Ho^{III}, Tm^{III}$, and Yb^{III} , while for $Ln^{III} = Ce^{III}, Nd^{III}$, and Sm^{III} the magnetic exchange interaction is antiferromagnetic.¹⁹ Matsumoto et al.'s investigations of tetranuclear complexes also showed that the magnetic interaction between Cu^{II} and Gd^{III}, Tb^{III} , and Dy^{III} ions is ferromagnetic.²⁰

The situation for other 3d metal ions is much less documented.²¹ The exchange interaction in the $Ni^{II}-Ln^{III}$ pair has not been studied as extensively as that of the $Cu^{II}-Ln^{III}$ pair, because many of the Ni^{II} 3d–4f complexes contained a square-planar Ni^{II} ion which is diamagnetic.²² However, for Schiff-based complexes, the $Ni^{II}-Ln^{III}$ exchange interaction seems to follow the same trend as the $Cu^{II}-Ln^{III}$ one, i.e., antiferromagnetic for the $4f^{1-5}$ ions and ferromagnetic for the $4f^{7-9}$ ions.²³

Besides model compounds to investigate magnetic phenomena, bimetallic 3d–4f Schiff-base complexes are interesting molecular modules for the construction of supramolecular systems.²⁴ We have been using such $[Cu^{II}Ln^{III}]$ and $[Ni^{II}Ln^{III}]$ units for the preparation of polynuclear architectures by assemblage with paramagnetic cyanometallate linkers (i.e., $\{Fe(CN)_6\}^{3-}$, $\{Mo(CN)_8\}^{3-}$, $\{W(CN)_8\}^{3-}$).²⁵ One of the aims of that approach was the construction of SMMs and SCMs by taking advantage of both the anisotropy of the Ln^{III} ions and the significant exchange interaction that may take place between the 3d ion of the Schiff-base complex and the cyanometallate. In this respect, the $[Ni^{II}Ln^{III}]$ units appeared well suited because of the significant ferromagnetic exchange with Mo^V and W^V .²⁶ While SMM

Scheme 1. Synthetic Pathway for $[Ni(valpn)(H_2O)_2]$



behaviors have been obtained, an evaluation of the gain that results from such arrays of exchange coupled $[Ni^{II}Tb^{III}]$ and $[Ni^{II}Dy^{III}]$ units was hindered by the absence of information for the simple bimetallic compounds. Herein, we report on the AC susceptibility behaviors for $[Ni(valpn)Ln(NO_3)_3]$ with $Ln = Tb^{III}$ and Dy^{III} ($valpn = 1,3$ -propanediyl-bis(2-iminomethylene-6-methoxy-phenol); Scheme 1). Moreover, the rather facile growth of crystals for the whole series of Ln ions (except radioactive promethium) allowed for solving of the structures for 10 complexes revealing differences only in solvent content and/or nitrate-anion coordination. The magnetic behaviors for all of the complexes have been investigated. The availability of the homologous $[Zn^{II}(valpn)Ln^{III}]$ derivatives (see preceding paper in this issue) prompted us to compare the magnetic data for the two families of compounds in order to emphasize the nature of magnetic interaction between Ni^{II} and the Ln^{III} ions in this ligand set.

EXPERIMENTAL SECTION

General Procedures and Materials. The chemicals used, i.e., *o*-vanillin, 1,3-diaminopropane, $Ni(NO_3)_2 \cdot 6H_2O$, and $Ln(NO_3)_3 \cdot xH_2O$, as well as all of the solvents (THF, acetonitrile) were of reagent grade and were purchased from commercial sources.

Synthesis of $[Ni(valpn)(H_2O)_2]$. 1,3-Diaminopropane (0.83 mL, 10 mmol) was added dropwise to a solution of *o*-vanillin (3.04 g; 20 mmol) in THF (50 mL), followed by NEt_3 (2.79 mL, 20 mmol). After 30 min, an aqueous solution (50 mL) containing $Ni(NO_3)_2 \cdot 6H_2O$ (2.91 g, 10 mmol) was added, and the resulting mixture was stirred for 1 h, while pouring in 200 mL of H_2O . A pale green solid was obtained, which was vacuum filtered and dried in the air ($m = 2.83$ g, $Y = 65\%$). Elemental analyses were used to characterize the starting material.

Synthesis of $[Ni(valpn)Ln^{III}]$ Complexes. $Ln(NO_3)_3 \cdot xH_2O$ (4 mmol) in MeCN (10 mL) was added to a suspension of $[Ni(valpn)(H_2O)_2]$ (0.17 g; 4.0 mmol) in MeCN (20 mL). The reaction mixture was stirred for about 30 min. Crystals of the desired compounds were obtained in high yields through the slow evaporation of the solvent over a period of a few days. This technique yielded crystals suitable for X-ray diffraction studies.

Crystallography. X-ray diffraction data for the crystals were collected on an IPDS II STOE diffractometer (compounds 1, 3, and 4), on a Bruker Apex2 diffractometer (compounds 2, 5, 11, and 12), on an IPDS I STOE diffractometer (compounds 7, and 8), or on an Xcalibur Oxford Diffraction diffractometer (compound 9), using graphite-monochromated Mo K α radiation sources ($\lambda = 0.71073$ Å). Multiscan absorption corrections were applied. The structures were solved by direct methods using SHELXS-97, SIR92, or SUPERFLIP and refined by means of least-squares procedures using the programs of the PC version of CRYSTALS or SHELXL-97. Atomic scattering factors were taken from the international tables for X-ray crystallography. Hydrogen atoms were included but not refined. Drawings of

Table 1. Crystal Data and Refinement for the Compounds 1–13

compound	1	2	3	4	5
formula	C ₂₃ H ₂₆ N ₇ O ₁₃ NiLa	C ₄₈ H ₆₃ N ₁₅ O ₃₀ Ni ₂ Ce ₂	C ₂₃ H ₂₆ N ₇ O ₁₃ NiPr	C ₄₆ H ₅₃ N ₁₄ O _{27.5} Ni ₂ Nd ₂	C ₂₅ H ₃₁ N ₈ O ₁₄ NiSm
<i>M</i> (g mol ⁻¹)	806.13	1727.77	808.13	1647.90	876.68
temp (K)	293(2)	180	293(2)	293(2)	295
wavelength (Å)	0.71073	0.71073	0.71073	0.71073	0.71073
cryst syst	monoclinic	monoclinic	monoclinic	orthorhombic	orthorhombic
space group	<i>P</i> ₂ ₁ / <i>n</i>	<i>P</i> ₂ ₁ / <i>c</i>	<i>P</i> ₂ ₁ / <i>n</i>	<i>Pbca</i>	<i>P</i> ₂ ₁ 2 ₁
<i>a</i> (Å)	9.8448(3)	17.9538(6)	9.8353(3)	18.4138(5)	12.5639(5)
<i>b</i> (Å)	17.4207(7)	11.3152(4)	17.3914(7)	19.6726(3)	14.7667(6)
<i>c</i> (Å)	18.2862(5)	32.2403(11)	18.1987(6)	35.2354(8)	19.3364(9)
α (deg)	90.00	90.00	90.00	90.00	90.00
β (deg)	91.570(2)	90.983(3)	91.811(3)	90.00	90.00
γ (deg)	90.00	90.00	90.00	90.00	90.00
<i>V</i> (Å ³)	3134.97(18)	6548.7(4)	3111.33(19)	12763.9(5)	3587.4(3)
<i>Z</i>	4	4	4	8	4
<i>D</i> _c	1.708	1.752	1.725	1.711	1.623
μ (mm ⁻¹)	2.017	2.028	2.225	2.273	2.217
<i>F</i> (000)	1608	3472	1616	6552	1748
goodness of fit	1.109	1.104	1.073	1.047	1.020
refinement on	<i>F</i> ²	<i>F</i>	<i>F</i> ²	<i>F</i> ²	<i>F</i>
final <i>R</i> ₁ , <i>wR</i> ₂	0.0433, 0.0766	0.0429, 0.0381	0.0480, 0.0942	0.0655, 0.1605	0.0355, 0.0357
[<i>I</i> > <i>nσ</i> (<i>I</i>)]	<i>n</i> = 2	<i>n</i> = 3	<i>n</i> = 2	<i>n</i> = 2	<i>n</i> = 3
<i>R</i> ₁ , <i>wR</i> ₂ (all data)	0.0698, 0.0834	0.0694, 0.0448	0.0772, 0.1028	0.0945, 0.1854	0.0502, 0.0391
largest diff. peak and hole (eÅ ⁻³)	0.369, -1.140	2.12, -0.83	0.519, -1.790	1.349, -1.336	2.88, -0.71
compound	7	8	9	11	12
formula	C ₂₅ H ₂₉ N ₈ O ₁₃ NiGd	C ₂₃ H ₃₆ N ₇ O ₁₈ NiTb	C ₂₃ H ₃₆ N ₇ O ₁₈ NiDy	C ₂₅ H ₂₉ N ₈ O ₁₃ NiEr	C ₃₈ H ₅₈ N ₈ O ₃₀ Ni ₂ Yb ₂
<i>M</i> (g mol ⁻¹)	865.52	916.22	919.79	875.52	1570.40
temp (K)	180	180	180	180	180
wavelength (Å)	0.71073	0.71073	0.71073	0.71073	0.71073
cryst syst	monoclinic	monoclinic	monoclinic	monoclinic	monoclinic
space group	<i>P</i> ₂ ₁ / <i>a</i>	<i>P</i> ₂ ₁ / <i>c</i>	<i>P</i> ₂ ₁ / <i>c</i>	<i>P</i> ₂ ₁ / <i>c</i>	<i>P</i> ₂ ₁ / <i>c</i>
<i>a</i> (Å)	23.8100(17)	13.5488(11)	13.5166(2)	13.1659(4)	11.1489(4)
<i>b</i> (Å)	10.4107(8)	10.4531(6)	10.4131(2)	10.4172(3)	17.1833(7)
<i>c</i> (Å)	13.2080(10)	24.351(2)	24.2996(5)	23.6189(6)	15.3045(7)
α (deg)	90.00	90.00	90.00	90.00	90.00
β (deg)	89.727(9)	98.710(10)	98.669(2)	91.1440(10)	108.659(2)
γ (deg)	90.00	90.00	90.00	90.00	90.00
<i>V</i> (Å ³)	3273.9(4)	3409.0(5)	3381.1(1)	3238.73(16)	2777.9(2)
<i>Z</i>	4	4	4	4	2
<i>D</i> _c	1.756	1.785	1.806	1.795	1.877
μ (mm ⁻¹)	2.658	2.696	2.837	3.230	4.100
<i>F</i> (000)	1724	1840	1844	1740	1556
goodness of fit	1.060	0.896	1.111	1.097	1.086
refinement on	<i>F</i> ²	<i>F</i> ²	<i>F</i>	<i>F</i>	<i>F</i>
final <i>R</i> ₁ , <i>wR</i> ₂	0.0457, 0.1238	0.0244, 0.0480	0.0241, 0.0232	0.0251, 0.0236	0.0307, 0.0318
[<i>I</i> > <i>nσ</i> (<i>I</i>)]	<i>n</i> = 2	<i>n</i> = 2	<i>n</i> = 3	<i>n</i> = 3	<i>n</i> = 2
<i>R</i> ₁ , <i>wR</i> ₂ (all data)	0.0552, 0.1300	0.0378, 0.0501	0.0301, 0.0244	0.0425, 0.0323	0.0578, 0.0578
largest diff. peak and hole (eÅ ⁻³)	1.14 - 2.07	0.66, -1.03	1.13, -1.37	1.07, - 0.73	2.06, - 0.79

the molecule were performed with the program Diamond 3. A summary of the crystallographic data and the structure refinement parameters is given in Table 1. CCDC reference numbers are as follows: 813327 (2), 813328 (5), 813329 (7), 813330 (8), 813331 (9), 813332 (11), 815089 (1), 815090(3), 815091(4), and 815749(12).

Magnetic Studies. Magnetic data were obtained with a Quantum Design MPMS-5 SQUID susceptometer. All samples consisted of crushed crystals dispersed in grease to avoid orientation in the field. Magnetic susceptibility measurements were performed in the 2–300 K temperature range in a 0.1 T applied magnetic field; diamagnetic

corrections were applied by using Pascal's constants.²⁷ Isothermal magnetization measurements were performed up to 5 T at 2 K. The magnetic susceptibilities have been computed by exact calculations of the energy levels associated with the spin Hamiltonian through diagonalization of the full matrix with a general program for axial and rhombic symmetries.²⁸ Least-squares fittings were accomplished with an adapted version of the function-minimization program MINUIT.²⁹

RESULTS AND DISCUSSION

A series of 13 $[\text{Ni}^{\text{II}}\text{Ln}^{\text{III}}]$ complexes was synthesized by the reaction of stoichiometric amounts of $[\text{Ni}(\text{valpn})(\text{H}_2\text{O})_2]$ and

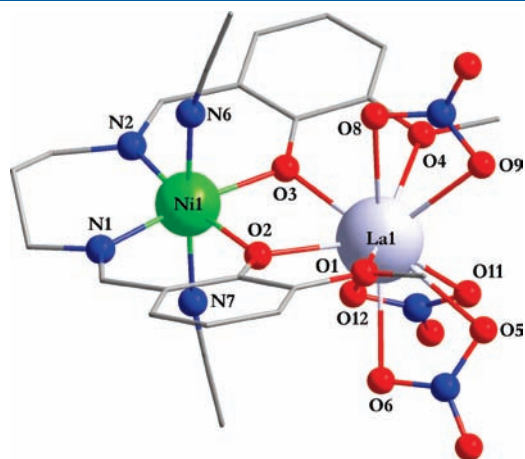


Figure 1. View of the molecular structure for $[\text{Ni}(\text{CH}_3\text{CN})_2(\text{valpn})\text{La}(\text{NO}_3)_3]$, **1**. Selected bond lengths (Å): Ni1–N1 = 2.020(2), Ni1–N2 = 2.040(2), Ni1–O2 = 2.053(2), Ni1–O3 = 2.032(2) Å, Ni1–N6 = 2.120(3), Ni1–N7 = 2.139(2) Å, La1–O1 = 2.701(2), La1–O2 = 2.412(2), La1–O3 = 2.4394(2), La1–O4 = 2.645(2) Å, La1–O5 = 2.641(2), La1–O6 = 2.576(2), La1–O8 = 2.631(2), La1–O9 = 2.570(2), La1–O11 = 2.685(2), La1–O12 = 2.632(2).

$\text{Ln}(\text{NO}_3)_3$. All, except the Yb derivative, are the anticipated bimetallic $[\text{Ni}(\text{valpn})\text{Ln}(\text{NO}_3)_3]$ complexes ($\text{Ln} = \text{La}^{\text{III}}\text{--Er}^{\text{III}}$, **1–11**), the formulas of which are completed by solvent molecules. For Yb, a tetranuclear compound, $[\text{Ni}(\text{H}_2\text{O})_2(\text{valpn})\text{Yb}(\text{NO}_3)(\mu_2\text{-OH})_2(\text{NO}_3)_2]$ (**12**), was obtained. The structures for all of the compounds have been confirmed by X-ray diffraction studies.

Crystal Structures. Six different structure types have been identified from the crystal data for the dinuclear compounds **1–11**. The structures' determinations revealed four different organizations for the bimetallic moieties. They are modulated mainly by the involvement of different solvent molecules (H_2O , MeCN) and by the linkages of the NO_3^- anions. Below, they have been classified as types I–IV, corresponding each to a given structure for the bimetallic unit. Type I is subdivided in three parts to reflect the solvent molecules found in the crystal lattice.

Type I.1. $[\text{Ni}(\text{CH}_3\text{CN})_2(\text{valpn})\text{Ln}(\text{NO}_3)_3]$: La (**1**), Pr (**3**)

Type I.2. $[\text{Ni}(\text{CH}_3\text{CN})_2(\text{valpn})\text{Ln}(\text{NO}_3)_3] \cdot \text{CH}_3\text{CN} \cdot 2\text{H}_2\text{O}$: Sm (**5**)

Type I.3. $[\text{Ni}(\text{CH}_3\text{CN})_2(\text{valpn})\text{Ln}(\text{NO}_3)_3] \cdot \text{CH}_3\text{CN}$: Eu (**6**), Gd (**7**), Er (**11**)

Type II. $[\text{Ni}(\text{CH}_3\text{CN})_2(\text{valpn})\text{Ce}(\text{NO}_3)_3(\text{H}_2\text{O})][\text{Ni}(\text{CH}_3\text{CN})(\text{H}_2\text{O})(\text{valpn})\text{Ce}(\text{NO}_3)_2(\text{H}_2\text{O})] \cdot \text{NO}_3 \cdot 2\text{CH}_3\text{CN}$: Ce (**2**)

Type III. $[\text{Ni}(\text{CH}_3\text{CN})_2(\text{valpn})\text{Nd}(\text{NO}_3)_3][\text{Ni}(\text{CH}_3\text{CN})(\text{H}_2\text{O})(\text{valpn})\text{Nd}(\text{NO}_3)_3] \cdot \text{CH}_3\text{CN} \cdot 0.5\text{H}_2\text{O}$: Nd (**4**)

Type IV. $[\text{Ni}(\text{CH}_3\text{CN})(\text{H}_2\text{O})(\text{valpn})\text{Ln}(\text{NO}_3)(\text{H}_2\text{O})_3] \cdot 2\text{NO}_3 \cdot \text{CH}_3\text{CN} \cdot \text{H}_2\text{O}$: Tb (**8**), Dy (**9**)

Compounds **1**, **3**, **5–7**, and **11** belong to type I and possess the same structural organization for the bimetallic unit. They differ only by the solvent molecules found in the lattice. Compound **1** will be briefly described as representative. The geometrical features for the other compounds are given in Tables S1 and S2 from the Supporting Information section.

The lanthanum derivative crystallizes in the $P2_1/n$ monoclinic space group and consists of neutral $[\text{Ni}(\text{CH}_3\text{CN})_2(\text{valpn})\text{La}(\text{NO}_3)_3]$ entities (Figure 1). The nickel ion displays an

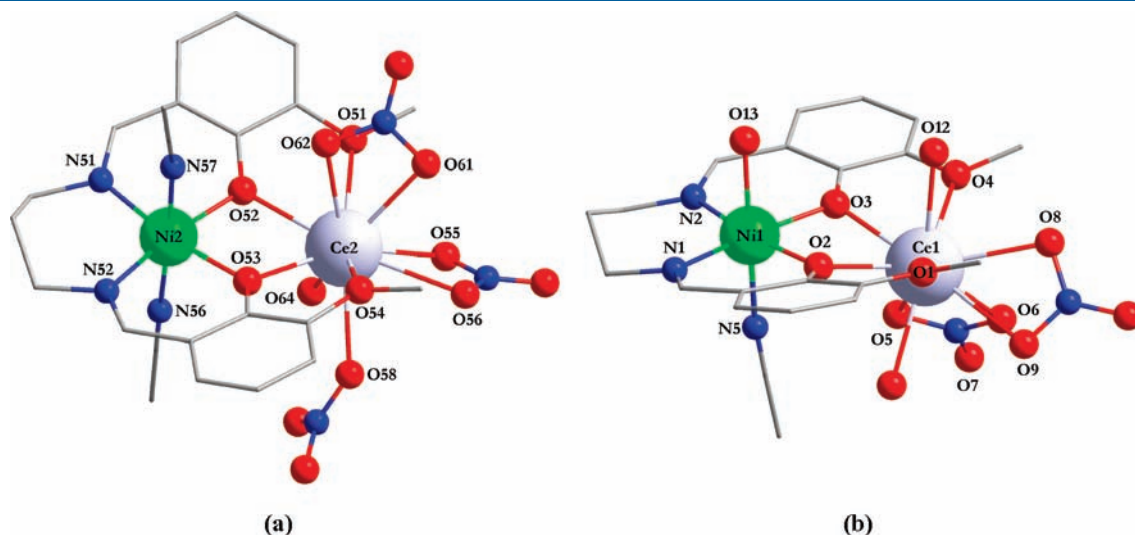


Figure 2. View of the molecular structure for (a) $[\text{Ni}(\text{CH}_3\text{CN})_2(\text{valpn})\text{Ce}(\text{NO}_3)_3(\text{H}_2\text{O})]$ and (b) $[\text{Ni}(\text{CH}_3\text{CN})(\text{H}_2\text{O})(\text{valpn})\text{Ce}(\text{NO}_3)_2(\text{H}_2\text{O})_2]^+$ entities of **2**. Selected bond lengths (Å): (a) Ni2–N51 = 2.032(2), Ni2–N52 = 2.049(2), Ni2–N56 = 2.113(2), Ni2–N57 = 2.150(3), Ni2–O52 = 2.0477(18), Ni2–O53 = 2.0302(18), Ce2–O12 = 2.520(2), Ce2–O51 = 2.6568(17), Ce2–O52 = 2.4656(17), Ce2–O53 = 2.4164(18), Ce2–O54 = 2.6037(18), Ce2–O55 = 2.610(2), Ce2–O56 = 2.676(2), Ce2–O58 = 2.565(2), Ce2–O61 = 2.582(2), Ce2–O62 = 2.644(2), Ce2–O64 = 2.479(2) Å. (b) Ni1–N1 = 2.027(2), Ni1–N2 = 2.043(2), Ni1–N5 = 2.116(2), Ni1–O2 = 2.0382(17), Ni1–O3 = 2.0263(17), Ni1–O13 = 2.1329(19), Ce1–O1 = 2.6692(18), Ce1–O2 = 2.4169(17), Ce1–O3 = 2.4624(18), Ce1–O4 = 2.6738(18), Ce1–O5 = 2.625(2), Ce1–O6 = 2.632(2), Ce1–O8 = 2.589(2), Ce1–O9 = 2.691(2), Ce1–O11 = 2.505(2) Å.

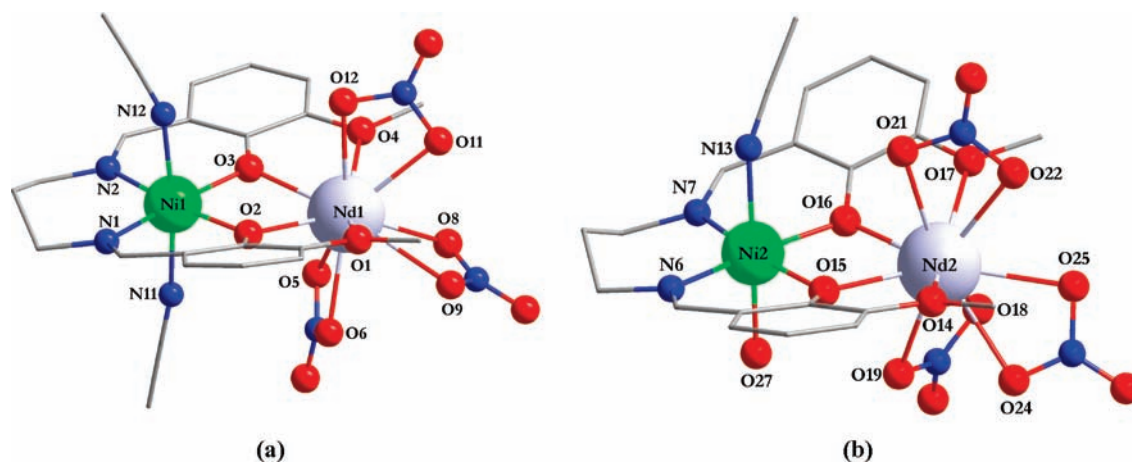


Figure 3. View of the molecular structure for the (a) $[\text{Ni}(\text{CH}_3\text{CN})_2(\text{valpn})\text{Nd}(\text{NO}_3)_3]$ and (b) $[\text{Ni}(\text{CH}_3\text{CN})(\text{H}_2\text{O})(\text{valpn})\text{Nd}(\text{NO}_3)_3]$ molecular units of 4. Selected bond lengths (Å): (a) Ni1–N1 = 2.028(4), Ni1–N2 = 2.046(4), Ni1–N11 = 2.128(4), Ni1–N12 = 2.163(5), Ni1–O2 = 2.036(3), Ni1–O3 = 2.017(3), Nd1–O1 = 2.619(3), Nd1–O2 = 2.401(3), Nd1–O3 = 2.397(3), Nd1–O4 = 2.579(3), Nd1–O5 = 2.583(4), Nd1–O6 = 2.508(5), Nd1–O8 = 2.565(4), Nd1–O9 = 2.644(4), Nd1–O11 = 2.524(4), Nd1–O12 = 2.571(4). (b) Ni2–N6 = 2.018(4), Ni2–N7 = 2.037(4), Ni2–N13 = 2.167(4), Ni2–O15 = 2.041(3), Ni2–O16 = 2.034(3), Ni2–O27 = 2.120(4), Nd2–O14 = 2.545(3), Nd2–O15 = 2.396(3), Nd2–O16 = 2.386(3), Nd2–O17 = 2.557(3), Nd2–O18 = 2.592(5), Nd2–O19 = 2.590(5), Nd2–O21 = 2.563(4), Nd2–O22 = 2.570(5), Nd2–O24 = 2.604(4), Nd2–O25 = 2.574(4).

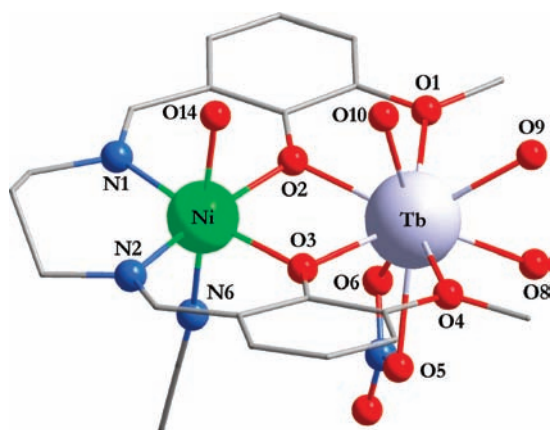


Figure 4. View of the molecular structure for $[\text{Ni}(\text{CH}_3\text{CN})(\text{H}_2\text{O})(\text{valpn})\text{Tb}(\text{NO}_3)_3(\text{H}_2\text{O})_3]^+$, 8. Selected bond lengths (Å): Ni–N1 = 2.030(3), Ni–N2 = 2.021(3), Ni–N6 = 2.114(3), Ni–O2 = 2.025(2), Ni–O3 = 2.027(2), Ni–O14 = 2.168(2), Tb–O1 = 2.488(2), Tb–O2 = 2.307(2), Tb–O3 = 2.318(2), Tb–O4 = 2.487(2), Tb–O5 = 2.509(2), Tb–O6 = 2.469(2), Tb–O8 = 2.452(2), Tb–O9 = 2.351(2), Tb–O10 = 2.436(2).

octahedral environment, with a N_2O_2 equatorial plane built by the donor atoms of the organic ligand and two apical acetonitrile ligands. The lanthanum ion is located in the open compartment, being surrounded by 10 oxygen atoms. Two phenolato and two methoxy oxygen atoms arise from the Schiff base, and two oxygen atoms arise from each of the three chelating nitrate ions.

Compound 2 has a type II structure and crystallizes in the $P2_1/c$ monoclinic space group. One neutral $[\text{Ni}(\text{CH}_3\text{CN})_2(\text{valpn})\text{Ce}(\text{NO}_3)_3]$ complex (Figure 2a) and one monocationic $[\text{Ni}(\text{CH}_3\text{CN})(\text{H}_2\text{O})(\text{valpn})\text{Ce}(\text{NO}_2)_2(\text{H}_2\text{O})_2]^+$ bimetallic unit (Figure 2b) are found in the crystal lattice together with an uncoordinated nitrate ion and solvent molecules.

Within the neutral entity, the nickel ion has an octahedral environment consisting of a N_2O_2 equatorial plane formed by the

donor atoms of the Schiff-base ligand and two apical acetonitrile ligands. The cerium ion is surrounded by 10 oxygen atoms comprising two phenolato and two methoxy oxygen atoms from the Schiff-base, four oxygen atoms arising from the two chelating nitrate anions, the oxygen atom of one terminal nitrate ligand, and the oxygen atom from one aqua ligand.

Within the monocationic $[\text{Ni}(\text{CH}_3\text{CN})(\text{H}_2\text{O})(\text{valpn})\text{Ce}(\text{NO}_3)_2(\text{H}_2\text{O})]^+$ unit, the hexacoordinated nickel ion is surrounded by the organic ligand in the equatorial positions and in apical positions by one MeCN and one H_2O ligand. As for the neutral unit, the cerium ion is 10-coordinated with the four oxygen atoms of the Schiff-base ligand, four oxygen atoms belonging to two chelating nitrate anions, and by two H_2O ligands.

The third structural type is represented by the neodymium derivative, $[\text{Ni}(\text{CH}_3\text{CN})_2(\text{valpn})\text{Nd}(\text{NO}_3)_3][\text{Ni}(\text{CH}_3\text{CN})(\text{H}_2\text{O})(\text{valpn})\text{Nd}(\text{NO}_3)_3] \cdot \text{CH}_3\text{CN} \cdot 0.5\text{H}_2\text{O}$ (4) that crystallizes in the $Pbca$ orthorhombic space group. Two neutral dinuclear $[\text{Ni}(\text{valpn})\text{Ln}(\text{NO}_3)_3]$ units are found in the crystal lattice, together with solvent molecules. The complexes differ by the nature of the ligands in apical positions of the Ni centers, i.e., two MeCN or one MeCN and one H_2O , respectively (Figure 3).

Within the $[\text{Ni}(\text{CH}_3\text{CN})_2(\text{valpn})\text{Nd}(\text{NO}_3)_3]$ units, the nickel ion shows an octahedral environment, with a N_2O_2 tetragonal base formed by the donor atoms of the organic ligand, and two apical acetonitrile ligands. The Nd^{III} ion fills the open compartment, and it is coordinated by the 10 oxygen atoms from the Schiff-base and from the three chelating nitrate anions. The $[\text{Ni}(\text{CH}_3\text{CN})(\text{H}_2\text{O})(\text{valpn})\text{Nd}(\text{NO}_3)_3]$ entity has a similar structure but with the Ni^{II} ion coordinated by an aqua ligand and by an acetonitrile molecule in apical positions.

Complexes 8 and 9 belong to the type IV structures with the general formula $[\text{Ni}(\text{CH}_3\text{CN})(\text{H}_2\text{O})(\text{valpn})\text{Ln}(\text{NO}_3)(\text{H}_2\text{O})_3](\text{NO}_3)_2(\text{CH}_3\text{CN})(\text{H}_2\text{O})$. They crystallize in the $P2_1/c$ monoclinic space group. The terbium derivative, 8, consists of a cationic $[\text{Ni}(\text{CH}_3\text{CN})(\text{H}_2\text{O})(\text{valpn})\text{Tb}(\text{NO}_3)(\text{H}_2\text{O})_3]^{2+}$ unit, two uncoordinated nitrate anions, one H_2O , and one MeCN molecule (Figure 4).

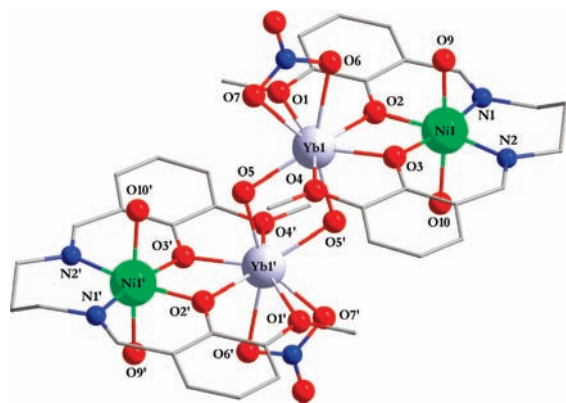


Figure 5. View of the molecular structure for $[\text{Ni}(\text{H}_2\text{O})_2(\text{valpn})\text{Yb}(\text{NO}_3)(\mu_2\text{-OH})_2]$. Selected bond lengths (Å): Ni–N1 = 2.026(3), Ni–N2 = 2.029(3), Ni–O2 = 2.026(2), Ni–O3 = 2.0160(19), Ni–O9 = 2.120(2), Ni–O10 = 2.114(2), Yb1–O1 = 2.440(2), Yb1–O2 = 2.2484(19), Yb1–O3 = 2.2541(19), Yb1–O4 = 2.419(2), Yb1–O5 = 2.159(2), Yb1–O5' = 2.199(2), Yb1–O6 = 2.431(3), Yb1–O7 = 2.438(2) ($' = 1 - x, -y, -z$).

The Ni^{II} center has an octahedral surrounding with an acetonitrile and an aqua ligand in the apical positions. The Tb^{III} ion is surrounded by nine oxygen atoms arising from the Schiff-base ligand, from the chelating nitrate ion, and from three aqua ligands.

Surprisingly, the Yb^{III} derivative, **12**, is not strictly a dinuclear complex, such as those obtained with the other Ln^{III} ions, but a dimer of hydroxo-bridged bimetallic units. This compound crystallizes in the monoclinic space group $P2_1/c$ and consists of tetranuclear $[\text{Ni}(\text{H}_2\text{O})_2(\text{valpn})\text{Yb}(\text{O}_2\text{NO})(\mu_2\text{-OH})_2]^{2+}$ units, two uncoordinated nitrate ions, and lattice H_2O molecules. A view of the tetranuclear aggregate is given in Figure 5.

The centrosymmetric tetranuclear cationic units are constructed by connecting two $\{\text{Ni}(\text{H}_2\text{O})_2(\text{valpn})\text{Yb}(\text{NO}_3)\}$ fragments via two hydroxo bridges. Within each fragment the nickel ions are hexacoordinated, the apical positions being occupied by the aqua ligands. Each ytterbium ion is eight-coordinated by four oxygen atoms arising from the organic ligand, the chelating nitrate, and the two hydroxo bridges. The intramolecular $\text{Yb}\cdots\text{Yb}$ distance is 3.549 Å.

Selected bond distances for compounds **1–5**, **7–9**, **11**, and **12** are given in the Supporting Information.

Comparison of the structures found for **1–12** shows that whereas the coordination sphere of the Ni ions remains the same, the surroundings of the Ln ions show some degree of change from La to Yb. This can be ascribed to the size of the ions, which decreases from the left to the right of the Ln series, hence the tendency of replacing η^2 -coordinated NO_3^- anions with sterically less demanding H_2O ligands. However, it can be noticed that the structure with three NO_3^- 's coordinated to the Ln applies over the whole first half of the series (i.e., for $4f^0$ to $4f^7$ ions). This surrounding was also found for the $4f^{11}$ ion Er, suggesting that the ionic radii may not be the only parameter to direct the coordination preferences.

The access to the bimetallic complexes with the almost whole series of Ln ions, and the availability of their $[\text{Zn}^{\text{II}}\text{Ln}^{\text{III}}]$ homologues, suggested the possibility of gathering information on the exchange interaction operative between Ni^{II} and Ln^{III} ions for a large set of complexes with very similar structures. Therefore, the magnetic properties for compounds **1–12** have been investigated.

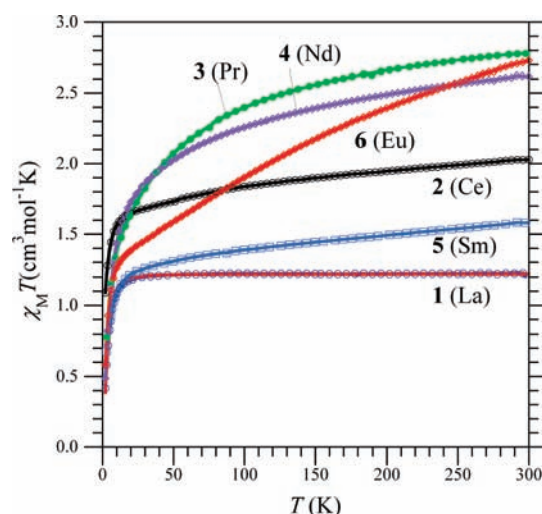


Figure 6. Experimental and calculated temperature dependence of $\chi_M T$ for compounds **1–6**. The red line represents the calculated behavior for **1**.

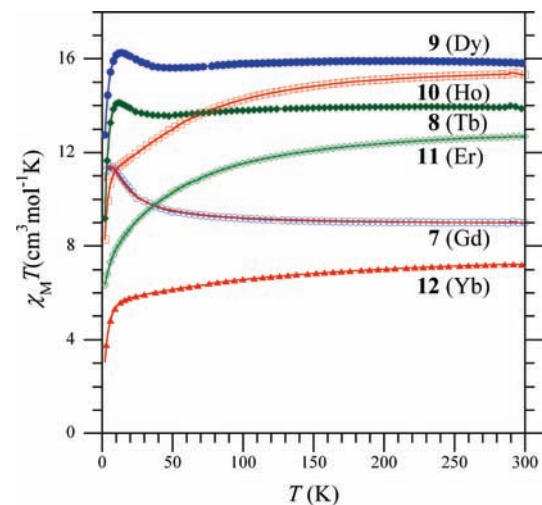


Figure 7. Temperature dependence of $\chi_M T$ for compounds **7–12**. For **7**, the red line corresponds to the calculated behavior (see text).

Magnetic Properties. The molar magnetic susceptibility, χ_M , for compounds **1–12** has been recorded in the temperature range 2–300 K (Figures 6 and 7). Let us start with the simple cases of the La and Gd derivatives, **1** and **7**. For these compounds, the deviation from Curie behavior is due to the ZFS associated with Ni^{II} (for **1**) and to the exchange interaction operative between Ni^{II} and Gd^{III} for **7**. For both compounds, these parameters can be easily evaluated by modeling the magnetic behaviors. The temperature dependence of $\chi_M T$ for **1** is represented in Figure 6. At 300 K, the value of $\chi_M T$ is $1.22 \text{ cm}^3 \text{ mol}^{-1} \text{ K}$, in agreement with the contribution of one Ni^{II} ion. This value remains unchanged down to ca. 30 K and decreases below to reach $0.42 \text{ cm}^3 \text{ mol}^{-1} \text{ K}$ at 2 K. For Gd derivative **7** (Figure 7), the value of $\chi_M T$ at 300 K is $9.0 \text{ cm}^3 \text{ mol}^{-1} \text{ K}$, in good agreement with the contribution of noninteracting Ni^{II} and Gd^{III} centers. This value steadily increases as T is lowered to reach $11.40 \text{ cm}^3 \text{ mol}^{-1} \text{ K}$ at 5 K revealing a ferromagnetic $\text{Ni}^{\text{II}}\text{–Gd}^{\text{III}}$ interaction. These magnetic behaviors have been modeled (see the Experimental

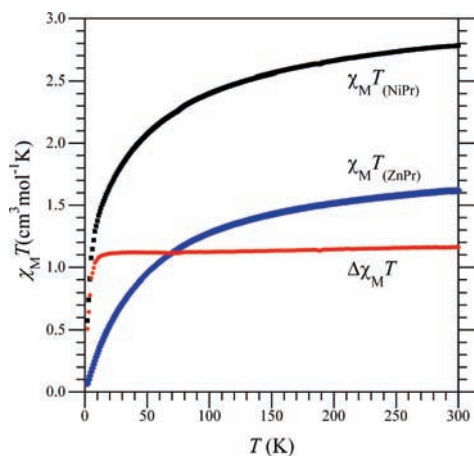


Figure 8. Temperature dependence of $\chi_M T_{(\text{NiPr})}$ (black ■) and $\chi_M T_{(\text{ZnPr})}$ (blue ■), for the $[\text{Ni}^{\text{II}}\text{Pr}^{\text{III}}]$ and $[\text{Zn}^{\text{II}}\text{Pr}^{\text{III}}]$ complexes, and the difference $\Delta\chi_M T$ (red ●).

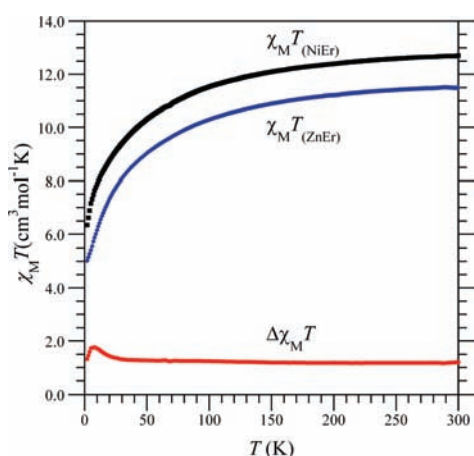


Figure 9. Temperature dependence of $\chi_M T_{(\text{NiEr})}$ (black ■) and $\chi_M T_{(\text{ZnEr})}$ (blue ■), for the $[\text{Ni}^{\text{II}}\text{Er}^{\text{III}}]$ and $[\text{Zn}^{\text{II}}\text{Er}^{\text{III}}]$ complexes, and the difference $\Delta\chi_M T$ (red ●).

Section), with the best fit yielding for **1** $D = 8.6 \text{ cm}^{-1}$ and $g = 2.21$ and, for **7**, $J_{\text{NiGd}} = 2.3 \text{ cm}^{-1}$ (based on isotropic Hamiltonian $H = -J_{\text{Ni}} \mathbf{S}_{\text{Ni}} \cdot \mathbf{S}_{\text{Gd}}$), $D = 7.5 \text{ cm}^{-1}$, $g = 2.0$, and $zJ' = -0.11 \text{ cm}^{-1}$, where J and J' are the intra- and intermolecular exchange coupling parameters, respectively. The value of the ferromagnetic interaction, J_{NiGd} is close to the one reported by Costes et al. for a dinuclear complex with a similar ligand ($+3.6 \text{ cm}^{-1}$).^{10c} The exchange interaction between phenoxo-bridged Ni^{II} and Gd^{III} ions was found to be ferromagnetic with several other complexes, the values of the J parameter spanning from ~ 0.2 to $\sim 5 \text{ cm}^{-1}$.^{10,23,25}

For the other complexes, the magnetic properties are more complicated because of the intervening first-order angular momentum and crystal field effect for the Ln^{III} ions. For these compounds, the variation of the magnetic behavior arises from the superposition of two phenomena. One is the result of the exchange interaction between the Ni^{II} and Ln^{III} ions. The second is intrinsic to the Ln^{III} ion and originates from the thermal population of the so-called Stark levels.³⁰ This phenomenon is modulated by the crystal field and the symmetry of the compound, and there is no easy-to-handle analytical model to account for this

contribution. However, rather facile access to qualitative information on the exchange interaction is possible by simple comparison of the magnetic behaviors for the exchange coupled system and for a homologous complex with Ln^{III} as the only paramagnetic component.^{8c,15,17,31}

The nature of the exchange interaction between Ni^{II} , in our case, and lanthanides displaying spin–orbit coupling can be emphasized by the general procedure that consists of representing the temperature dependence of the difference $\Delta\chi_M T = \chi_M T_{(\text{NiLn})} - \chi_M T_{(\text{ZnLn})}$, where the intrinsic magnetic behavior of the lanthanide ions, as found within the dinuclear $[\text{Zn}^{\text{II}}\text{Ln}^{\text{III}}]$ complexes (see preceding paper in this issue), is subtracted from the one measured for the $[\text{Ni}^{\text{II}}\text{Ln}^{\text{III}}]$ complexes. In Figures 8 and 9 are shown the results obtained by this procedure for the Pr^{III} and Er^{III} derivatives, examples for antiferromagnetic and ferromagnetic $[\text{Ni}^{\text{II}}\text{Ln}^{\text{III}}]$ interactions, respectively. The temperature dependences of $\chi_M T_{(\text{NiLn})}$, $\chi_M T_{(\text{ZnLn})}$, and $\Delta\chi_M T$ for all of the other compounds can be found in the Supporting Information.

The $\chi_M T$ for both the $[\text{Ni}^{\text{II}}\text{Pr}^{\text{III}}]$, **3**, and $[\text{Zn}^{\text{II}}\text{Pr}^{\text{III}}]$ derivatives steadily decreases when T is lowered. The difference, $\Delta\chi_M T = \chi_M T_{(\text{NiPr})} - \chi_M T_{(\text{ZnPr})}$, is characterized by a value that remains unchanged between 300 and 30 K and in agreement with the contribution of solely one Ni^{II} . Below this temperature, a sharp decrease of $\Delta\chi_M T$ is observed, revealing the occurrence of an antiferromagnetic interaction between Ni^{II} and Pr^{III} for compound **3**. A related feature is found for the other paramagnetic Ln ions of the first half of the 4f series, indicating that antiferromagnetic interactions take place between Ni^{II} and Ln^{III} for $\text{Ln} = \text{Ce} - \text{Sm}$, i.e., compounds **2–5**.

For compounds **7–9**, the increase exhibited by $\chi_M T$ at low temperatures unambiguously reveals the existence of ferromagnetic interactions between Ni^{II} and the Ln^{III} ions. Such a feature is not found for Ho^{III} and Er^{III} derivatives **10** and **11**; for these compounds, $\chi_M T$ steadily decreases with T . As mentioned above, such behavior does not allow for a conclusion on the exchange interaction taking place between the metal centers. Indeed, the intrinsic contribution of these ions might simply compensate the increase of $\chi_M T$ resulting from a ferromagnetic interaction.^{15b} This is exactly what occurs for **11**, as shown in Figure 9. When the contribution of the Er^{III} ion, $\chi_M T_{(\text{ZnEr})}$, is subtracted from the $\chi_M T_{(\text{NiEr})}$ behavior of **11**, the ferromagnetic interaction between Ni^{II} and Er^{III} is clearly revealed by the temperature dependence of $\Delta\chi_M T$. The same has been found for the Ho^{III} derivative **10**.

This qualitative evaluation of the exchange interactions established between Ni^{II} and paramagnetic Ln^{III} ions clearly shows that antiferromagnetic interactions take place with the ions with less than half-filled 4f orbitals, i.e., for Ce^{III} to Sm^{III} , whereas the interaction is ferromagnetic for the ions of the second half, from Gd^{III} to Er^{III} . These results are in agreement with earlier reports on $[\text{Ni}^{\text{II}}\text{Ln}^{\text{III}}]$ Schiff-base complexes.²³ They also follow the trend established for related $[\text{Cu}^{\text{II}}\text{Ln}^{\text{III}}]$ compounds.^{15–20}

The $\chi_M T$ behavior for the tetranuclear compound **12** was also investigated (Figure 7). At 300 K, the value for $\chi_M T$ is $7.22 \text{ cm}^3 \text{mol}^{-1} \text{K}$, in agreement with the contributions of two Yb^{III} ($2.57 \text{ cm}^3 \text{mol}^{-1} \text{K}$) and two Ni^{II} ions. This value gradually diminishes for lower temperatures with a sharp decrease below 20 K to reach $3 \text{ cm}^3 \text{mol}^{-1} \text{K}$ for 2 K. Unfortunately, the homologous tetranuclear $[\text{Zn}^{\text{II}}\text{Yb}^{\text{III}}]$ derivative was not available for performing the qualitative evaluation of the exchange interaction between Ni^{II} and Yb^{III} .

Finally, AC susceptibility measurements have been performed for derivatives **8**, **9**, and **10** in order to investigate the possible

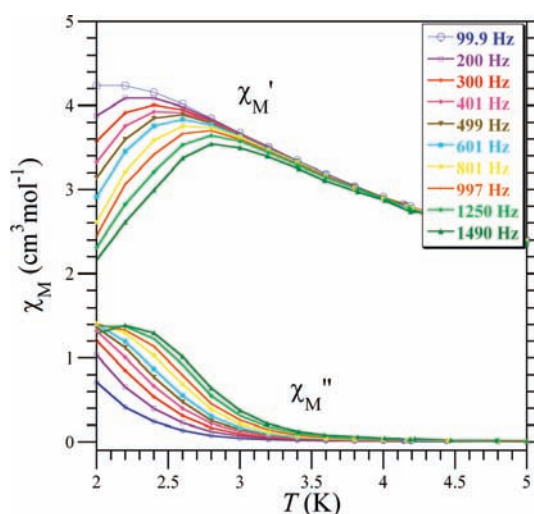


Figure 10. Temperature dependence of the in-phase (χ_M') and out-of-phase (χ_M'') signals for **9**, at different frequencies of the oscillating field ($H_{DC} = 1$ kOe).

slow relaxation of their magnetization. In the absence of an applied field, no signal was found for the imaginary part of the magnetic susceptibility down to 2 K. However, with an applied static field of $H_{DC} = 1000$ Oe, the onset of a χ_M'' signal is observed with the Tb^{III} derivative **8** above 2 K (Supporting Information). For the Dy^{III} derivative **9**, χ_M'' deviates from zero below 4 K and is frequency dependent (Figure 10). Unfortunately, a maximum for the χ_M'' curves is seen above 2 K only for the highest frequency investigated, 1490 Hz, which impeded confirmation of a SMM-type behavior. Nevertheless, the behavior observed for **9** clearly suggests that such a simple bimetallic $[Ni^{II}Dy^{III}]$ complex may already behave as a SMM, much like what has been observed for a related $[Cu^{II}Tb^{III}]$ derivative.^{5a} It is interesting to recall also that the SMM behavior of compound **9** is preserved in a tetranuclear complex and in a 1-D coordination polymer, which result by connecting dinuclear $[Ni^{II}Dy^{III}]$ nodes with dicarboxylato spacers.^{24d}

Concluding Remarks. Bimetallic 3d–4f Schiff-base complexes are widely used and can be considered as rather common species, in part due to their facile preparation. Surprisingly, these are often involved in the construction of more complex molecular architectures with limited information on the physical properties of the bimetallic unit itself. This knowledge, however, is particularly important when the goal is to design a system with improved properties. In this respect, spin ground state, magnetic anisotropy, and slow relaxation are of prime importance in magnetic systems. For bimetallic 3d–4f Schiff-base complexes, these features will hugely vary as a function of the Ln^{III} ion. For the $[Ni^{II}Ln^{III}]$ derivatives investigated here, we provided a set of magnetic properties for almost the whole Ln series, i.e., from La^{III} to Er^{III} , that have allowed for an emphasis on the occurrence of antiferromagnetic Ni^{II} – Ln^{III} interaction for the Ln^{III} ions for the beginning of the 4f series, and ferromagnetic interactions starting from gadolinium toward the end of the series.

Most of the paramagnetic Ln^{III} ions are characterized by an anisotropic moment, but the strength of this magnetic moment at low temperatures varies significantly along the series. The strongest moments are found for the Tb^{III} and Dy^{III} ions, which make them valuable candidates for the design of nanomagnets.

The AC susceptibility for the $[Ni^{II}(valpn)Tb^{III}]$ and $[Ni^{II}(valpn)Dy^{III}]$ complexes reveals that slow relaxation of their magnetization can already be observed around 2 K for these strictly dinuclear compounds. The holmium derivative, **10**, does not show frequency dependent in-phase and out-of-phase magnetic susceptibilities.

■ ASSOCIATED CONTENT

S Supporting Information. Synthetic and experimental details, crystallographic data, and supplementary magnetic data. AC magnetic susceptibility measurements for compound **8**. This material is available free of charge via the Internet at <http://pubs.acs.org>

■ AUTHOR INFORMATION

Corresponding Author

*E-mail: sutter@lcc-toulouse.fr, marius.andruh@dnt.ro.

■ ACKNOWLEDGMENT

Financial support from the CNCSIS (grant IDEI 506/2009) and the Agence Universitaire de la Francophonie (grant to FZC) are gratefully acknowledged.

■ REFERENCES

- (1) (a) Kahn, O. *Struct. Bond. (Berlin)* **1987**, 68, 89. (b) Kahn, O. *Adv. Inorg. Chem.* **1995**, 43, 179.
- (2) (a) Kahn, O. *Molecular Magnetism*; VCH: New York, 1993. (b) Kahn, O.; Galy, J.; Journaux, Y. *J. Am. Chem. Soc.* **1982**, 104, 2165. (c) Pei, Y.; Verdaguer, M.; Kahn, O.; Sletten, J.; Renard, J.-P. *J. Am. Chem. Soc.* **1986**, 108, 428.
- (3) Bencini, A.; Benelli, C.; Caneschi, A.; Carlin, R. L.; Dei, A.; Gatteschi, D. *J. Am. Chem. Soc.* **1985**, 107, 8128.
- (4) Gatteschi, D.; Sessoli, R.; Villain, J. *Molecular Nanomagnets*; Oxford University Press: New York, 2006.
- (5) (a) Costes, J.-P.; Dahan, F.; Wernsdorfer, W. *Inorg. Chem.* **2006**, 45, 5. (b) Kajiwara, T.; Nakano, M.; Takaishi, S.; Yamashita, M. *Inorg. Chem.* **2008**, 47, 8604. (c) Costes, J.-P.; Vendier, L.; Wernsdorfer, W. *Dalton Trans.* **2010**, 39, 4886.
- (6) Costes, J.-P.; Dahan, F.; Dupuis, A.; Laurent, J. P. *Inorg. Chem.* **1996**, 35, 2400.
- (7) (a) Bencini, A.; Benelli, C.; Caneschi, A.; Dei, A.; Gatteschi, D. *Inorg. Chem.* **1986**, 25, 572. (b) Benelli, C.; Caneschi, A.; Gatteschi, D.; Guillou, O.; Pardi, L. *Inorg. Chem.* **1990**, 29, 1750. (c) Guillou, O.; Bergerat, P.; Kahn, O.; Bakalbassis, E.; Boubekur, K.; Batail, P.; Guillot, M. *Inorg. Chem.* **1992**, 31, 110. (d) Andruh, M.; Ramade, I.; Codjovi, E.; Guillou, O.; Kahn, O.; Trombe, J. C. *J. Am. Chem. Soc.* **1993**, 115, 1822. (e) Ramade, I.; Kahn, O.; Jeannin, Y.; Robert, F. *Inorg. Chem.* **1997**, 36, 930. (f) Costes, J.-P.; Dahan, F.; Dupuis, A. *Inorg. Chem.* **2000**, 39, 5994. (g) Sanz, J. L.; Ruiz, R.; Gleizes, A.; Lloret, F.; Faus, J.; Julve, M. *Inorg. Chem.* **1996**, 35, 7384. (h) Benelli, C.; Gatteschi, D. *Chem. Rev.* **2002**, 102, 2369.
- (8) (a) Andruh, M.; Costes, J.-P.; Diaz, C.; Gao, S. *Inorg. Chem.* **2009**, 48, 3342. (b) Sakamoto, M.; Manseki, K.; Okawa, H. *Coord. Chem. Rev.* **2001**, 219–221, 379. (c) Sutter, J.-P.; Kahn, M. L. In *Magnetism: Molecule to materials*; Miller, J. S., Drillon, M., Eds.; Wiley-VCH: Weinheim, Germany, 2005; Vol. 5, p 161.
- (9) (a) Costes, J.-P.; Dahan, F.; Donnadiou, B.; Garcia-Tojal, J.; Laurent, J. P. *Eur. J. Inorg. Chem.* **2001**, 363. (b) Costes, J.-P.; Dupuis, A.; Laurent, J. P. *J. Chem. Soc., Dalton Trans.* **1998**, 735.
- (10) (a) Brechin, E. K.; Harris, S. G.; Parsons, S.; Winpenny, R. E. P. *J. Chem. Soc., Dalton Trans.* **1997**, 1665. (b) Winpenny, R. E. P. *Chem. Soc. Rev.* **1998**, 27, 447. (c) Costes, J.-P.; Dahan, F.; Dupuis, A.; Laurent, J. P. *Inorg. Chem.* **1997**, 36, 4284. (d) Lisowski, J.; Starynowicz, P. *Inorg. Chem.* **1999**, 38, 1351. (e) Costes, J. P.; Vendier, L. *Eur. J. Inorg. Chem.* **2010**, 2768.

- (11) (a) Costes, J.-P.; Dahan, F.; Dupuis, A.; Laurent, J. P. *C. R. Acad. Sci., Ser. IIc: Chim.* **1998**, *1*, 417. (b) Brayshaw, P. A.; Bunzli, J.-C. G.; Froidevaux, P.; Harrowfield, J. M.; Kim, Y.; Sobolev, A. N. *Inorg. Chem.* **1995**, *34*, 2068. (c) Rigault, S.; Piguët, C.; Bernardinelli, G.; Hopfgartner, G. *J. Chem. Soc., Dalton Trans.* **2000**, 4587. (d) Ma, B. Q.; Gao, S.; Bai, O.; Sun, H. L.; Xu, G. X. *J. Chem. Soc., Dalton Trans.* **2000**, 1003. (e) Costes, J. P.; Clemente-Juan, J. M.; Dahan, F.; Dumestre, F.; Garcia-Tojal, J.; Tuchagues, J. P. *Chem.—Eur. J.* **2002**, *8*, 5430.
- (12) Sanada, T.; Suzuki, T.; Yoshida, T.; Kaizaki, S. *Inorg. Chem.* **1998**, *37*, 4712.
- (13) (a) Costes, J.-P.; Dupuis, A.; Laurent, J. P. *Eur. J. Inorg. Chem.* **1998**, 1543. (b) Edder, C.; Piguët, C.; Bunzli, J.-C. G.; Hopfgartner, G. *Chem.—Eur. J.* **2001**, *7*, 3014. (c) Costes, J. P.; Clemente-Juan, J. M.; Dahan, F.; Dumestre, F.; Tuchagues, J. P. *Inorg. Chem.* **2002**, *41*, 2886.
- (14) (a) Costes, J. P.; Dahan, F.; Dupuis, A.; Laurent, J. P. *Inorg. Chem.* **2000**, *39*, 169. (b) Stoian, S. A.; Paraschiv, C.; Kiritsakas, N.; Lloret, F.; Munck, E.; Bominaar, E. L.; Andruh, M. *Inorg. Chem.* **2010**, *49*, 3387. (c) Costes, J. P.; Vendier, L. *C. R. Chim.* **2010**, *13*, 661. (d) Lescop, C.; Luneau, D.; Belorisky, E.; Fries, P.; Guillot, M.; Rey, P. *Inorg. Chem.* **1999**, *38*, 5472. (e) Caneschi, A.; Dei, A.; Gatteschi, D.; Sorace, L.; Vostrikova, K. *Angew. Chem., Int. Ed.* **2000**, *39*, 246. (f) Figuerola, A.; Diaz, C.; Ribas, J.; Tangoulis, V.; Granell, J.; Lloret, F.; Mahia, J.; Maestro, M. *Inorg. Chem.* **2003**, *42*, 641.
- (15) (a) Kahn, M. L.; Mathoniere, C.; Kahn, O. *Inorg. Chem.* **1999**, *38*, 3692. (b) Sutter, J.-P.; Kahn, M. L.; Kahn, O. *Adv. Mater.* **1999**, *11*, 863. (c) Kahn, M. L.; Sutter, J.-P.; Golhen, S.; Guionneau, P.; Ouahab, L.; Kahn, O.; Chasseau, D. *J. Am. Chem. Soc.* **2000**, *122*, 3413.
- (16) (a) Kahn, M. L.; Lecante, P.; Verelst, M.; Mathoniere, C.; Kahn, O. *Chem. Mater.* **2000**, *12*, 3073. (b) Kahn, M. L.; Ballou, R.; Porcher, P.; Kahn, O.; Sutter, J.-P. *Chem.—Eur. J.* **2002**, *8*, 525.
- (17) (a) Costes, J.-P.; Dahan, F.; Dupuis, A.; Laurent, J. P. *Inorg. Chem.* **1997**, *36*, 4284. (b) Costes, J.-P.; Dahan, F.; Dupuis, A.; Laurent, J.-P. *Chem.—Eur. J.* **1998**, *4*, 1616.
- (18) Shiga, T.; Ohba, M.; Ohkawa, H. *Inorg. Chem.* **2004**, *43*, 4435.
- (19) Koner, R.; Lin, H.-H.; Wei, H.-H.; Mohanta, S. *Inorg. Chem.* **2005**, *44*, 3524.
- (20) Kido, T.; Ikuta, Y.; Sunatsuki, Y.; Ogawa, Y.; Matsumoto, N.; Re, N. *Inorg. Chem.* **2003**, *42*, 398.
- (21) (a) Yamaguchi, T.; Costes, J.-P.; Kishima, Y.; Kojima, M.; Sunatsuki, Y.; Bréfuel, N.; Tuchagues, J.-P.; Vendier, L.; Wernsdorfer, W. *Inorg. Chem.* **2010**, *49*, 9125. (b) Costes, J.-P.; Garcia-Tojal, J.; Tuchagues, J.-P.; Vendier, L. *Eur. J. Inorg. Chem.* **2009**, 3801. (c) Chandrasekhar, V.; Pandian, B. M.; Azhakar, R.; Vittal, J. J.; Clérac, R. *Inorg. Chem.* **2007**, *46*, 5140.
- (22) (a) Lisowski, J.; Starynowicz, P. *Inorg. Chem.* **1999**, *38*, 1351. (b) Sanada, T.; Suzuki, T.; Kaizaki, S. *J. Chem. Soc., Dalton Trans.* **1998**, 959.
- (23) (a) Bayly, S. R.; Xu, Z.; Patrick, B. O.; Rettig, S. J.; Pink, M.; Thompson, R. C.; Orvig, C. *Inorg. Chem.* **2003**, *42*, 1576. (b) Barta, C. A.; Bayly, S. R.; Read, P. W.; Patrick, B. O.; Thompson, R. C.; Orvig, C. *Inorg. Chem.* **2008**, *47*, 2280. (c) Shiga, T.; Ito, N.; Hidaka, A.; Okawa, H.; Kitagawa, S.; Ohba, M. *Inorg. Chem.* **2007**, *46*, 3492. (d) Yamaguchi, T.; Sunatsuki, Y.; Ishida, H.; Kojima, M.; Akashi, H.; Re, N.; Matsumoto, N.; Pochaba, A.; Mrozinski, J. *Inorg. Chem.* **2008**, *47*, 5736. (e) Chandrasekhar, V.; Pandian, B. M.; Boomishankar, R.; Steiner, A.; Vittal, J. J.; Houry, A.; Clérac, R. *Inorg. Chem.* **2008**, *47*, 4918. (f) Costes, J. P.; Yamaguchi, T.; Kojima, M.; Vendier, L. *Inorg. Chem.* **2009**, *48*, 5555.
- (24) (a) Andruh, M. *Pure Appl. Chem.* **2005**, *77*, 1685. (b) Andruh, M. *Chem. Commun.* **2007**, 2565. (c) Andruh, M. *Chem. Commun.* **2011**, 47, 3025. (d) Pasatoiu, T. D.; Etienne, M.; Madalan, A. M.; Andruh, M.; Sessoli, R. *Dalton Trans.* **2010**, 39, 4802. (e) Madalan, A. M.; Avarvari, N.; Fourmigué, M.; Clérac, R.; Chibotaru, L. F.; Clima, S.; Andruh, M. *Inorg. Chem.* **2008**, *47*, 940. (f) Gheorghe, R.; Cucos, P.; Andruh, M.; Costes, J.-P.; Donnadiu, B.; Shova, S. *Chem.—Eur. J.* **2006**, *12*, 187.
- (25) (a) Sutter, J.-P.; Dhers, S.; Costes, J.-P.; Duhayon, C. *C. R. Chim.* **2008**, *11*, 1200. (b) Visinescu, D.; Madalan, A. M.; Andruh, M.; Duhayon, C.; Sutter, J.-P.; Ungur, L.; Van den Heuvel, W.; Chibotaru, L. F. *Chem.—Eur. J.* **2009**, *15*, 11808. (c) Dhers, S.; Sahoo, S.; Costes, J.-P.; Duhayon, C.; Ramasesha, S.; Sutter, J.-P. *CrystEngComm.* **2009**, *11*, 2078. (d) Sutter, J.-P.; Dhers, S.; Rajamani, R.; Ramasesha, S.; Costes, J.-P.; Duhayon, C.; Vendier, L. *Inorg. Chem.* **2009**, *48*, 5820. (e) Gheorghe, R.; Madalan, A. M.; Costes, J.-P.; Wernsdorfer, W.; Andruh, M. *Dalton Trans.* **2010**, 39, 4734.
- (26) Visinescu, D.; Desplanches, C.; Imaz, I.; Bahers, V.; Pradhan, R.; Villamena, F.; Guionneau, P.; Sutter, J.-P. *J. Am. Chem. Soc.* **2006**, *128*, 10202.
- (27) Pascal, P. *Ann. Chim. Phys.* **1910**, *19*, 5.
- (28) Boudalis, A. K.; Clemente-Juan, J.-M.; Dahan, F.; Tuchagues, J.-P. *Inorg. Chem.* **2004**, *43*, 1574.
- (29) James, F.; Roos, M. *Comput. Phys. Commun.* **1975**, *10*, 343.
- (30) Bünzli, J. C. G.; Chopin, G. R. In *Lanthanide Probes in Life, Chemical, and Earth Sciences: Theory and Practice*; Elsevier: Amsterdam, 1989.
- (31) Sutter, J.-P.; Kahn, M. L.; Mörtl, K. P.; Ballou, R.; Porcher, P. *Polyhedron* **2001**, 1593.